Soft trapping lasts longer: Dwell time of a Brownian particle varied by potential shape

Itsuo Hanasaki,[1,*] Takahiro Nemoto,[2] and Yoshito Y. Tanaka[3,4]

[1]*Institute of Engineering, Tokyo University of Agriculture and Technology, Naka-cho 2-24-16, Koganei, Tokyo 184-8588, Japan*

[2]*Philippe Meyer Institute for Theoretical Physics, Physics Department, École Normale Supérieure & PSL Research University, 24, rue Lhomond, 75231 Paris Cedex 05, France*

[3]*Institute of Industrial Science, The University of Tokyo, 4-6-1 Komaba, Meguro-ku, Tokyo 153-8505, Japan*

[4]*Japan Science and Technology Agency, PRESTO, 4-1-8 Honcho, Kawaguchi, Saitama 332-0012, Japan*

(Received 14 September 2018; revised manuscript received 14 December 2018; published 13 February 2019)

It is often regarded that the dwell time (or residence time, escape time, trapping duration) of trapped Brownian particles is described by the multiplication of two separate factors, i.e., the diffusive traveling time of the trapping domain size without taking into account the trapping force, and the stochastic event of overcoming the trapping energy by thermal one instantaneously. However, we show that the ratio of dwell time to the typical traveling time for the trapping domain size depends on the shape of the force field. The shape of the trapping potential affects this ratio even if the trapping energy gap is the same and the smooth potential has a single minimum. Our finding suggests the possible application of the potential shape to realize the desired trapping characteristics.

DOI: 10.1103/PhysRevE.99.022119

I. INTRODUCTION

It has long been recognized that the technology to precisely control the position of a nanoscale object is important for the progress of nanoscience and nanotechnology in general [1–4]. One of the typical techniques to achieve such control is optical trapping, where small particles with diameters less than or equal to micrometers can be trapped in space near the focus of a laser beam by the optical force based on the gradient of the electric field [5]. Optical trapping has found many applications in the physical and life sciences, ranging from single-molecule force measurements to optical particle sorting [6–11]. However, optical trapping of nanoparticles, especially smaller than 100 nm, is still challenging, because the gradient optical force becomes much weaker with the smaller particles, scaling with the third power of its size [12]. The main approach to stably trap nanoparticles has been to increase the laser intensity and consequently the depth of the trapping potential. In fact, the trapping techniques are not necessarily based on the optical principle, but there are some other principles, such as electrostatic fluidic trap [13], dielectrophoretic tweezer in microfluidic device [14], and Paul trap [15–17].

The escape event from the trapped state of a Brownian particle subject to the conservative force field with trapping energy $\Delta E(\geq 0)$ is often modeled by the Arrhenius-type equation, i.e., the simplest form of chemical reaction with the rate constant k_{TST} as follows [18–22]:

$$k_{\mathrm{TST}} = k_0 \exp\left(-\frac{\Delta E}{k_{\mathrm{B}}T}\right), \tag{1}$$

where k_{B} is the Boltzmann's constant, T is the absolute temperature, and k_0 corresponds to the rate constant without energy barrier, i.e., the travel of a particle subject to Brownian motion. This functional form is widely used in the context of stochastic event subject to thermal fluctuation, where traveling distance or duration by Brownian motion is negligible in the reaction event. With this assumption, the dwell time (or residence time, escape time, trapping duration) τ_{TST} is expressed as

$$\tau_{\mathrm{TST}} = \tau_0 \exp\left(\frac{\Delta E}{k_{\mathrm{B}}T}\right). \tag{2}$$

The timescale τ_0 is usually regarded as the characteristic for a Brownian particle with a diffusion coefficient D to travel a distance $d_{\mathrm{s}}/2$ from the bottom of potential to the boundary, which can be expressed as

$$\tau_0 = \frac{d_{\mathrm{s}}^2}{8D}, \tag{3}$$

considering that $\sqrt{2D\tau_0} = d_{\mathrm{s}}/2$. The diffusion coefficient of a spherical particle with a diameter d_{p} in a fluid with a viscosity η is described by the Stokes-Einstein relation as follows:

$$D = \frac{k_{\mathrm{B}}T}{3\pi\eta d_{\mathrm{p}}}, \tag{4}$$

and D is directly related to the friction coefficient γ by the Einstein relation as follows:

$$D = \frac{k_{\mathrm{B}}T}{\gamma}, \tag{5}$$

where the validity range of the Stokes-Einstein relation and linear Langevin picture in terms of molecular drag has been studied recently [23,24]. Equation (2) is widely used in the field of laser trapping or optical force on colloidal particles [18–22]. This equation indicates that the dwell time

*Corresponding author: hanasaki@cc.tuat.ac.jp

τ_d does not depend on the details of force field, but the energy difference ΔE alone. The trend of pursuit to achieve as high laser power as possible to realize the trapping of as small particle as possible originates from this picture of simplified mechanics. Depending on the situations, the higher laser power also cause heating of the medium [5], which is desired to be circumvented since it blurs the pure optical effect and sometimes undermines the functionality for biomedical applications [25,26].

However, the typical trapping force fields in reality have finite breadth of the trapping domain, and the trapped particles exhibit Brownian motion in the domain with finite time duration before escaping from it. Although the assumption of Eq. (2) does not take into account the finite spatiotemporal effect in terms of overcoming the energy difference, the particle climbs the force field with finite time, instead of instantaneously jumping the finite energy gap with infinite force and vanishing slope length. Therefore, we examine the validity range of this apparently oversimplified model through the numerical analysis. We show that there exists significant finite spatiotemporal effect of the trapping force field, which is promising for the stable trapping of smaller particles. If we look into each of the specific principle of trapping techniques, there are diversity in the factors that affects the dwell time. For example, nonconservative scattering force is also important in the case of laser trapping in the bulk environment. On the other hand, the effect of proximity to the solid wall in the fluid is also important in the case of electrostatic fluid trap in the nanochannel. Partly because of such diversity in specific situations, the basic and universal characteristics with respect to the conservative trapping force field in fluid has not been fully addressed. We focus on this common aspects of the role of force field on the dwell time of the Brownian particles.

II. MODEL AND METHODS

We consider the Brownian dynamics of particles suspended in fluid subject to trapping force field. The schematic diagram of the model system is shown in Fig. 1. The essential parameters that affects the dynamics is the trapping energy ΔE, the domain of this force field d_s, and the diameter d_p of the trapped particle. It should be noted that d_p affects only D through the Stokes-Einstein relation, i.e., Eq. (4). We assume that these parameters can be independently tuned, even if such a fine tuning is still challenging in laboratory experiments today.

As widely used in many literature and experimental data analysis [27], we employ the harmonic force field as follows [28]:

$$\Delta E(r) = \begin{cases} \dfrac{k_B T}{2\sigma^2} r^2 & (0 \le r \le d_s/2) \\ \dfrac{k_B T d_s^2}{8\sigma^2} & (r > d_s/2) \end{cases}, \tag{6}$$

where σ is the essential parameter that determines the trapping energy. To vary $\alpha \equiv \Delta E/k_B T$ without affecting the rest of the parameters, $\Delta E(r)$ for $r = d_s/2$ can be tuned through σ by

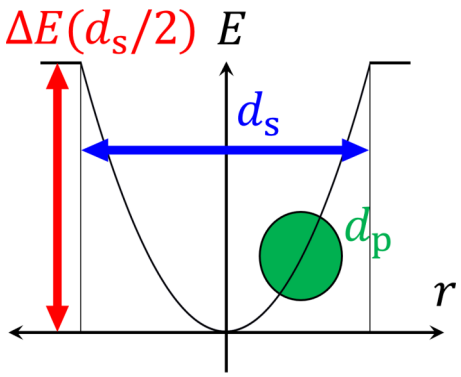

FIG. 1. Schematic diagram of the model system. A Brownian particle with a diameter d_p is suspended in a fluid. The particle is subject to a trapping force field of harmonic potential that depends only on the distance r with its origin defined at the minimum potential energy. The trapping force field acts in the finite domain with a width of d_s, and the trapping energy is denoted as $\Delta E(r)$. The escape event is judged with the position of the central position of the particle. d_p affects only the diffusion coefficient D through the Stokes-Einstein relation [cf. Eq. (4)].

$\Delta E = \alpha k_B T = k_B T (d_s/2)^2/(2\sigma^2)$ as follows:

$$\sigma = \frac{d_s}{2\sqrt{2\alpha}}. \tag{7}$$

We also examine the effect of the potential shape on the system characteristics by the variation of a single parameter n to define the simple potential energy function as follows:

$$\Delta E_n(r) = \frac{\alpha k_B T}{(d_s/2)^n} r^n, \tag{8}$$

where $n = 2$ corresponds to Eq. (6). The effect of potential steepness in the vicinity of the boundary $r = d_s/2$ can be varied by n without changing other parameters such as α and d_s. Namely, variation of d_s keeping $\Delta E(d_s/2)$ fixed leads to the variation of the spring constant k_s:

$$k_s = \frac{\alpha k_B T}{(d_s/2)^n}, \tag{9}$$

where $n = 2$ corresponds to the cases of Eq. (6). ΔE, d_s or k_s, and d_p are independent factors of the particle dynamics although it is still challenging to perform such an experiment using optical trapping based on current status of the technology.

The particle exhibits Brownian motion governed by the over-damped Langevin equation [28,29]:

$$\Delta r(t) \equiv r(t + \Delta t) - r(t) = \frac{f_c(r) D}{k_B T} \Delta t + \sqrt{2D\Delta t}\,\psi(t), \tag{10}$$

where $\Delta r(t)$ is the displacement at time t, D is the diffusion coefficient as mentioned in Eq. (4), $f_c(z)$ is the conservative force, Δt is the time step of the dynamics, and ψ is the normal random number. The force $f_c(r)$ is simply derived from the trapping energy:

$$f_c(r) = -\frac{\partial}{\partial r} \Delta E(r). \tag{11}$$

We numerically solve this equation [28,29] with a time resolution of ca. $\tau_0/\Delta t_{\rm dyn} = 10^6$, where $\Delta t_{\rm dyn}$ is the time step of numerical integration of the equation. The simulations are run until the number of the frames of $\Delta t_{\rm frm} = 10^{-2}$ s without any escaping event reaches 10^5, or the number of time steps reaches 10^{12}. The escaping event means the particle's stepping out of the force field domain with a width of $d_{\rm s}$. We define the ambient temperature $T = 298.15$ K and use the corresponding viscosity $\eta = 0.890 \times 10^{-3}$ P of water. The random number generator is the Box-Muller method. When the particle reaches the boundary of the force field, the position is initialized at the bottom of the potential (i.e., $r = 0$). The dwell time $\tau_{\rm d}$ is defined as the time required for (the center of) the particle to reach the boundary $r = d_{\rm s}/2$ of the trapping force field from its initial position $r = 0$.

III. RESULTS AND DISCUSSION

In fact, Eq. (10) can be nondimensionalized by employing the unit length scale of $d_{\rm s}/2$ and unit timescale of τ_0 [cf. Eq. (3)] as follows:

$$\begin{aligned}\Delta r^*(t^*) &\equiv r^*(t^* + \Delta t^*) - r^*(t^*) \\ &= -\tfrac{1}{2} n\alpha (r^*)^{n-1} \Delta t^* + \sqrt{\Delta t^*}\psi(t), \end{aligned} \tag{12}$$

where the specific form of the potential defined in Eq. (8) is taken into account. This dimensionless equation indicates that the system behavior is fundamentally determined by α and n. Hereafter, we examine how these parameters affect the dwell time $\tau_{\rm d}$. The dependence of the dwell time $\tau_{\rm d}$ on α and n is shown in Fig. 2. The dwell time is evaluated by the dimensionless form $\tau_{\rm d}/\tau_0$, which enables the essential characterization of α dependence without being affected by the growth of $\tau_{\rm d}$ by the mere increase of $d_{\rm s}$. Figure 2 clearly shows that $\tau_{\rm d}/\tau_0$ depends not only on α but also n. The actual $\tau_{\rm d}/\tau_0$ is always smaller than $\tau_{\rm TST}/\tau_0$. Larger $\tau_{\rm d}/\tau_0$ is realized for the smaller n.

According to the Arrhenius equation (Eq. (2)), the height of the potential should be the only factor to affect the dwell time irrespective of its shape. However, as seen in Fig. 2(a), the deviation from such classical formula is clearly observed. From the comparison of the data for different n, one can see that higher n results in smaller dwell times. This observation can be quantitatively rationalized using an analytical expression $\tau_{\rm A}$ to estimate the dwell time. Indeed, as detailed below, we derive the following expression:

$$\tau_{\rm A} = \tau_0\, {}_2F_2\left(\frac{2}{n}, 1; \frac{n+1}{n}, \frac{n+2}{n}; \alpha\right), \tag{13}$$

for any even number n, where ${}_2F_2$ is a generalized hypergeometric function. (A generalized hypergeometric function ${}_pF_q$ is defined as ${}_pF_q(a_1,\ldots,a_p;b_1,\ldots,b_q;z) = \sum_{m=0}^{\infty} \frac{(a_1)_m\cdots(a_p)_m}{(b_1)_m\cdots(b_q)_m}\frac{z^m}{m!}$, where $(a)_m$ is the Pochhammer symbol: $(a)_0 = 1$ and $(a)_n = a(a+1)(a+2)\cdots(a+n-1)$.) In Fig. 2(a), we plot this analytical expression $\tau_{\rm A}$ for $n = 2$ and 20, which show excellent agreements with the numerical simulations. The dependence of numerical errors on the time resolution of the simulation is shown in Fig. 3. The hypergeometric function ${}_2F_2$ has the following asymptotic form for large α:

$$ {}_2F_2\left(\frac{2}{n}, 1; \frac{n+1}{n}, \frac{n+2}{n}; \alpha\right) \sim \frac{2\Gamma(1/n)}{n^2\alpha^{1+1/n}} e^{\alpha}, \tag{14}$$

where $\Gamma(z)$ is the gamma function. (The gamma function is defined as $\Gamma(z) = \int_0^\infty t^{z-1}e^{-t}dt$.) The Arrhenius equation

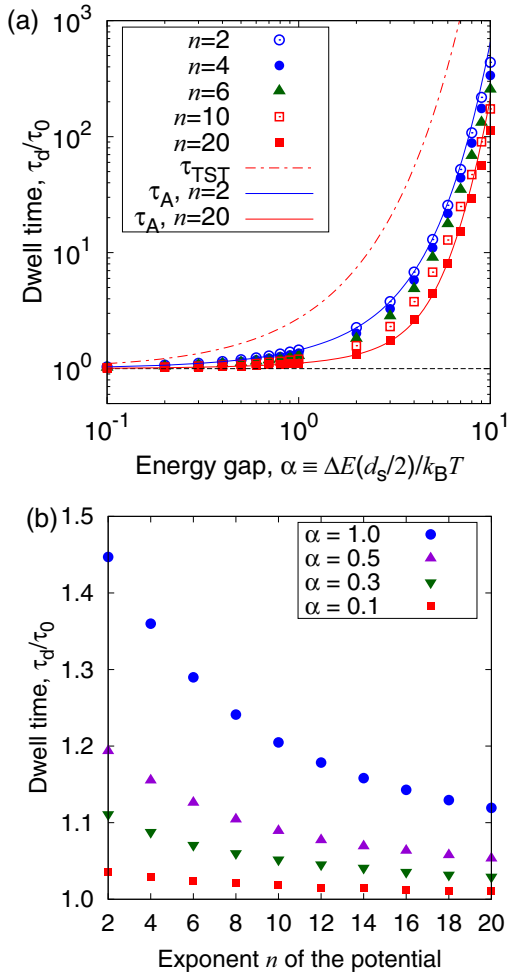

FIG. 2. Dependence of dwell time on (a) the trapping energy $\alpha \equiv \Delta E(d_{\rm s}/2)/(k_{\rm B}T)$ and (b) the potential shape represented by the exponent n of Eq. (8). $\tau_{\rm TST}$ and $\tau_{\rm A}$ correspond to Eqs. (2) and (13), respectively.

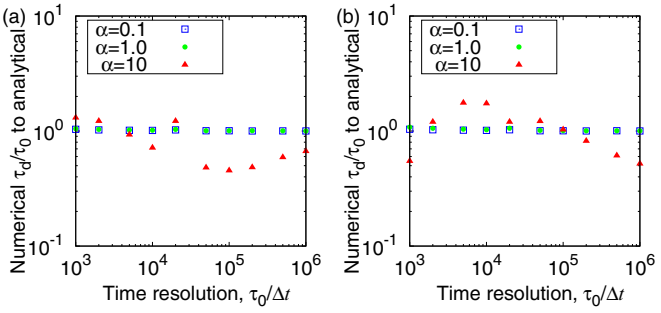

FIG. 3. Deviations of numerical results from analytical solution as a function of the time resolution when the exponent n of Eq. (8) is (a) 2 and (b) 20.

e^{α} is thus recovered as the leading term of this asymptotic form, showing the consistency between our result Eq. (13) and the classical Arrhenius equation. Note, however, that in the range of α that we consider in this paper, there are substantial deviations from the Arrhenius equation. To get an intuition how varying n affects these deviations, we take the large n limit in the hypergeometric function, which leads to

$$ {}_2F_2\left(\frac{2}{n}, 1; \frac{n+1}{n}, \frac{n+2}{n}; \alpha\right) = 1 + \frac{1}{n}g(\alpha) + O\left(\frac{1}{n^2}\right), \quad (15) $$

where $g(\alpha)$ consists of the derivatives of the hypergeometric function. (More precisely, $g(\alpha)$ is defined as $[2\ {}_2F_2^{(0,0;0,1)}(1,0;1,1;\alpha) + {}_2F_2^{(0,0;1,0)}(1,0;1,1;\alpha) + 2\ {}_2F_2^{(0,1;0,0)}(1,0;1,1;\alpha)]$, where ${}_2F_2^{(n_{a_1},n_{a_2};n_{b_1},n_{b_2})}(a_1,a_2;b_1,b_2;\alpha)$ is the $(n_{a_1},n_{a_2};n_{b_1},n_{b_2})$th-order partial derivative of ${}_2F_2(a_1,a_2;b_1,b_2;\alpha)$ by $(a_1,a_2;b_1,b_2)$, respectively.) This indicates that the dwell time converges to τ_0, which is the one without any trapping potential, as n increases: $\lim_{n\to\infty}\tau_A = \tau_0$. For a fixed potential height, softer the potential increases, much longer the particle can be trapped. In the large n limit, the potential barrier resembles a solid wall that might give an impression that the particle can be trapped longer. However, this is wrong: The particle can easily escape from such an extreme potential shape.

Next, we briefly explain how to derive the result Eq. (13). We use a well-known method to study the escape time of Brownian particles from a given domain. Since good textbooks to refer the detail of the derivation are largely available, we here only describe the outline of the derivation based on Ref. [30]. We first consider a probability density $P(r,t|r_0,0)$ of r at time t with the initial condition r_0 at time 0. The boundary conditions of $P(r,t|r_0,0)$ are absorbing boundary conditions $P(\pm d_s/2,t|r_0,0)=0$ or $P(r,t|\pm d_s/2,0)$, to describe our setup of simulations in which we reset the position of the particle each time it reaches the boundaries $r=\pm d_s/2$. Using this probability density $P(r,t|r_0,0)$, the probability that the particle still remains in the potential trap at time t is given as

$$ Q(r_0,t) \equiv \int_{-d_s/2}^{d_s/2} P(r,t|r_0,0)dr. \quad (16) $$

Since the derivative of $-Q(r_0,t)$ is the probability rate to escape the trap at time t, we get the escaping probability $R(r_0,t)dt$ during the time interval between t and $t+dt$ as $R(r_0,t)dt = -[\partial Q(r_0,t)/\partial t]dt$. By taking the integral of this escaping probability multiplied by t, we thus get an equation to describe the average *first-passage time*, $T(r_0) = \int_0^\infty tR(r_0,t)dt = \int_0^\infty Q(r_0,t)dt$. This means that once we know the time-evolution equation of the remaining probability $Q(r_0,t)$, we can get an equation to determine $T(r_0)$. Using the Fokker-Planck equation as such a time-evolution equation [30], the following ordinary differential equation is derived:

$$ \frac{f_c(r)D}{k_BT}\frac{dT(r)}{dr} + D\frac{d^2T(r)}{dr^2} = -1. \quad (17) $$

By solving this differential equation with boundary conditions $T(\pm d_s/2)=0$ and by noticing $T(0)=\tau_A$, we get Eq. (13).

It is worth addressing the sensitivity and numerical values between the relevant basic physical quantities under such circumstances. In particular, the spring constant k_s is an important property to link the intuition of many scientists and engineers engaged in experimental works to our numerical and analytical results. As far as we employ the definition of spring constant k_s in Eq. (9), the increase of n means that of k_s. If we consider the case of technologically realistic order of $d_s = 10^{-6}$ m, the numerical value of k_s is drastically varied by the variation of n, compared to the variation of α. In spite of this apparent numerical values, Fig. 2, τ_d/τ_0 is much more sensitive to α compared to n at first sight. However, the physically important range of α today is rather mainly close to the k_BT partly because of the available potential for smaller nanoparticles, and partly because of the relevance to the soft matter physics and biological context.

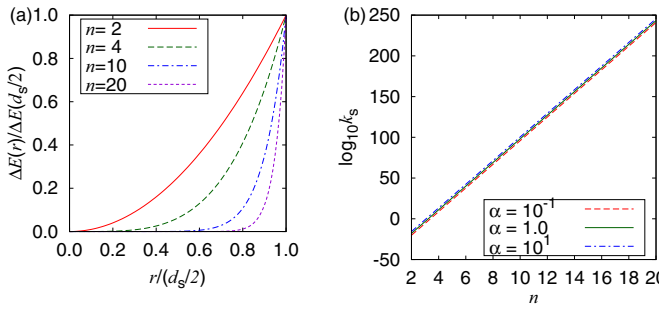

FIG. 4. Dependence of (a) potential shape and (b) generalized spring constant on the exponent n in Eqs. (8) and (9), respectively. The spring constant k_s in (b) is evaluated for the case where $d_s = 10^{-6}$ m.

The variation of n in Eq. (8) causes the variation of the functional shape of the potential and the generalized spring

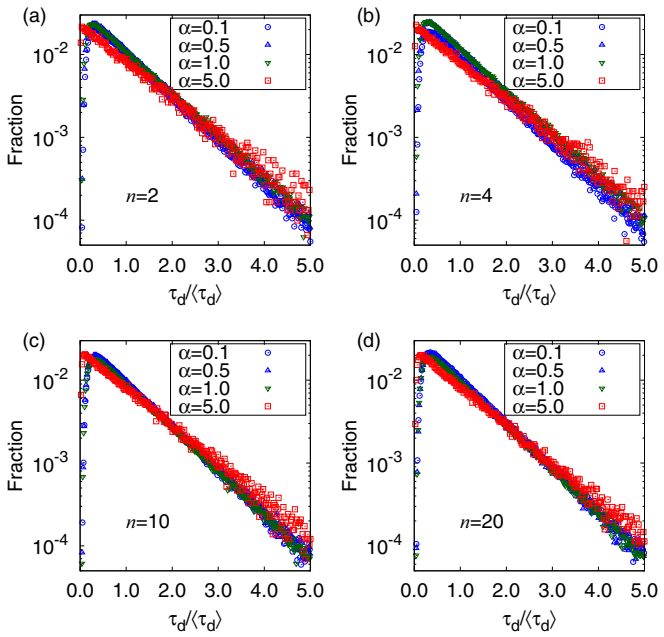

FIG. 5. Distribution of τ_d for different $\alpha \equiv \Delta E(d_s/2)/(k_BT)$ when the exponent n of the potential shape is (a) 2, (b) 4, (c) 10, and (d) 20, respectively. $\langle\tau_d\rangle$ indicates the average of τ_d for each combination of α and n.

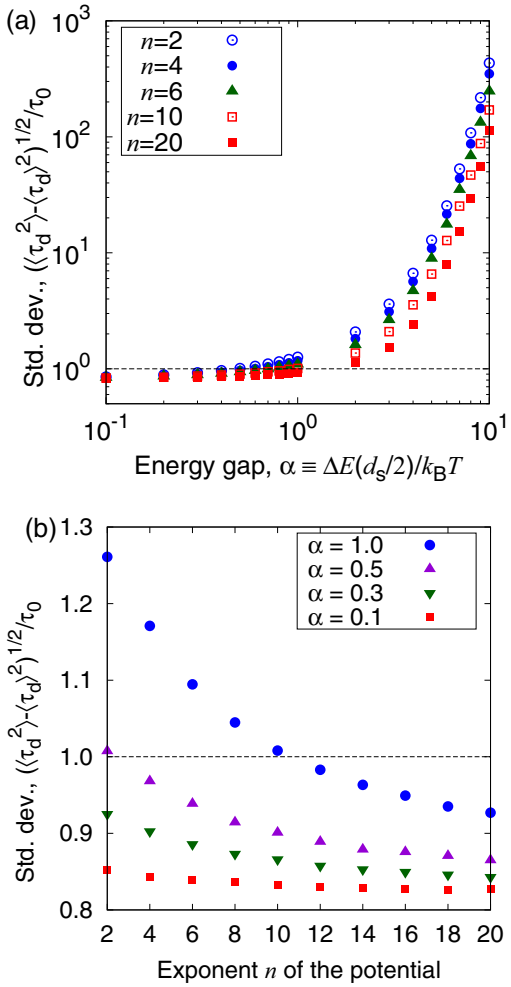

FIG. 6. Dependence of the standard deviation of the dwell time on (a) the trapping energy $\alpha \equiv \Delta E(d_s/2)/(k_B T)$ and (b) the potential shape represented by the exponent n of Eq. (8).

constant k_s of the potential as shown in Fig. 4. The larger n causes the steeper potential in the vicinity of $r = d_s/2$, whereas it is less steep in the vicinity of $r = 0$ as shown in Fig. 4(a). The larger spring constant for a linear spring corresponds to the stiffer spring. The variation of the spring constant with a fixed n is realized by α [Eq. (9)], but it corresponds to the increase of potential energy gap. The variation of d_s leads to that of the spring constant k_s as well. It leads to the increase of τ_0 but τ_d/τ_0 remains the same as far as α and n is kept constant. For example, k_s for the case of $n = 2$ does not affect τ_d/τ_0 as far as α is kept the same, although the variation of k_s by that of d_s causes the variation of both τ_d and τ_0. The dependence of τ_d/τ_0 on n is essentially important, considering the fact that Eq. (2) has long been employed in many situations of research without caring about the potential shape. Furthermore, it should also be noted that the potential shape depends on the specific systems of interest. Even within the case of laser trapping, the shape of the trapping potential depends on the specification of the laser [31].

Since the escape of the trapped Brownian particle is obviously the stochastic event, it is scattered around the mean dwell time. Therefore, we also examine the distribution of τ_d to understand the system characteristics by the numerical analysis. Figure 5 shows the distribution of τ_d scaled by its mean values for different combinations of α and n. The scaling of each result for (α, n) by the mean values almost collapse into a single curve. The peak is located at the values smaller than the mean, and the distribution beyond the peak value appears linear in the semilog plot. In other words, the probability distribution of $\tau_d/\langle\tau_d\rangle$ follows the exponential distribution for the most part, except for sufficiently small τ_d. The exponential distribution of the event indicates that the escape event of the particle originates from the probability that does not explicitly depend on time. The distributions also resembles those of Gumbel distribution. The Gumbel distribution often appears for the stochastic event of *extreme values*. In this case, the escape event takes place when sufficiently large displacement(s) by thermal fluctuation for a fixed $k_B T$ takes place. The same probability distribution when scaled by the mean value indicates that the breadths of distribution are wider for the cases with larger mean values $\langle\tau_d\rangle$. The standard deviation of the dwell time is important when evaluating its mean value from the experimental measurements. Figure 6 shows the dependence of the standard deviation of τ_d scaled by τ_0 on α and n. The standard deviation of τ_d/τ_0 drastically increases for large α (closer to 10^1), and it is smaller for large n. The sensitivity of this standard deviation to n grows with increasing α. In other words, the trend of the standard deviation of τ_d/τ_0 with respect to α and n is the same as the mean value of τ_d/τ_0 (cf. Fig. 2).

IV. CONCLUSIONS

We have shown both numerically and analytically that the dwell time is affected not only by the trapping energy but also by the force field shape. We have revealed that the smaller spring constant by smaller number of exponent in the polynomial potential function is advantageous for the longer dwell time when the trapping energy is the same. This is of fundamental importance in the application to the optical tweezers, and plasmon trapping in particular. The desired characteristics of optical force field to control crystallization [32] and those to trap a single particle precisely in a desired position are likely to be different. "Soft yet long" trapping may be preferred for the former situation compared to the "tight yet short" one. This specification is also likely to be more nontrivial when considering the capacity of the number of trapped particles.

ACKNOWLEDGMENTS

This work was partly supported by JSPS KAKENHI Grants No. 17H05463 and No. JP17H05462 in Scientific Research on Innovative Areas "Nano-Material Optical-Manipulation" and JST PRESTO Grant No. JPMJPR15PA, Japan.

[1] D. M. Eigler and E. K. Schweizer, Nature **344**, 524 (2000).
[2] O. M. Marago, P. H. Jones, P. G. Gucciardi, G. Volpe, and A. C. Ferrari, Nat. Nanotech. **8**, 807 (2013).
[3] Y. Tanaka, S. Kaneda, and K. Sasaki, Nano Lett. **13**, 2146 (2013).
[4] J. C. Ndukaife, A. V. Kildishev, A. G. A. Nnanna, V. M. Shalaev, S. T. Wereley, and A. Boltasseva, Nat. Nanotech. **11**, 53 (2016).
[5] A. Ashkin, J. M. Dziedzic, J. E. Bjorkholm, and S. Chu, Opt. Lett. **11**, 288 (1986).
[6] A. Ashkin, K. Schutze, J. M. Dziedzic, U. Euteneuer, and M. Schliwa, Nature **348**, 346 (1990).
[7] A. Ishijima and *et al.*, Cell **92**, 161 (1998).
[8] T. Imasaka, Y. Kawabata, T. Kaneta, and Y. Ishidzu, Anal. Chem. **67**, 1763 (1995).
[9] S. J. Hart and A. V. Terray, Appl. Phys. Lett. **83**, 5316 (2003).
[10] M. J. Lang, P. M. Fordyce, A. M. Engh, K. C. Neuman, and S. M. Block, Nat. Methods **1**, 133 (2004).
[11] J. W. Black, M. Kamenetska, and Z. Ganim, Nano Lett. **17**, 6598 (2017).
[12] B. T. Draine, Astrophys. J. **333**, 848 (1988).
[13] N. Mojarad and M. Krishnan, Nat. Nanotech. **7**, 448 (2012).
[14] M. Son, S. Choi, K. H. Ko, M. H. Kim, S. Lee, J. Key, Y. Yoon, I. S. Park, and S. W. Lee, Langmuir **32**, 922 (2016).
[15] W. Guan, S. Joseph, J. H. Park, S. Krstic, and M. A. Reed, Proc. Natl. Acad. Sci. U.S.A. **108**, 9326 (2011).
[16] J. H. Park and P. S. Krstic, Nanoscale Res. Lett. **7**, 156 (2012).
[17] J. H. Park, W. Guan, M. A. Reed, and P. S. Krstic, Small **8**, 907 (2012).
[18] K. Svoboda and S. M. Block, Opt. Lett. **19**, 930 (1994).
[19] C. Hosokawa, H. Yoshikawa, and H. Masuhara, Phys. Rev. E **72**, 021408 (2005).
[20] Y. Tanaka, H. Yoshikawa, and H. Masuhara, J. Phys. Chem. B **110**, 17906 (2006).
[21] M. Pelton, M. Liu, H. Y. Kim, G. Smith, P. Guyot-Sionnest, and N. F. Scherer, Opt. Lett. **31**, 2075 (2006).
[22] M. L. Juan, R. Gordon, Y. Pang, F. Eftekhari, and R. Quidant, Nat. Phys. **5**, 915 (2009).
[23] I. Hanasaki, R. Nagura, and S. Kawano, J. Chem. Phys. **142**, 104301 (2015).
[24] I. Hanasaki, D. Fujiwara, and S. Kawano, J. Chem. Phys. **144**, 094503 (2016).
[25] A. Ashkin and J. M. Dziedzic, Science **235**, 1517 (1987).
[26] Y. Liu, G. J. Sonek, M. W. Berns, and B. J. Tromberg, Biophys. J. **71**, 2158 (1996).
[27] P. M. Hansens, V. K. Bhatia, N. Harrit, and L. Oddershede, Nano Lett. **5**, 1937 (2005).
[28] I. Hanasaki, Y. Kazoe, and T. Kitamori, Microfluid. Nanofluid. **22**, 56 (2018).
[29] I. Hanasaki and J. H. Walther, Phys. Rev. E **96**, 023109 (2017).
[30] C. Gardiner, *Stochastic Methods*, 4th ed. (Springer, Berlin, 2009).
[31] T. Taira, Laser Rev. **26**, 723 (1998).
[32] T. Sugiyama, K. Yuyama, and H. Masuhara, Acc. Chem. Res. **45**, 1946 (2012).